

Shock Response Analysis of Blast Hardened Bulkhead in Naval Ship under Internal Blast

Sang-Gab Lee¹, Hwan-Soo Lee¹, Jae-Seok Lee¹, Yong Yook Kim², Gul Gui Choi²

¹Korea Maritime & Ocean University, Marine Safety Technology

²Korea Advanced Institute of Science and Technology

1 Abstract

It is necessary to restrict the damage area for the enhancement of ship survivability under the internal blast of a Semi-Armor Piercing (SAP) warhead inside a ship's compartment, and to develop design guidance and performance verification technique of Blast Hardened Bulkhead (BHB) for the protection of its damage diffusion to adjoining compartment and continuous flooding. The objective of this study is to develop shock response analysis technique of BHB under the internal blast using MMALE (Multi-Material Arbitrary Lagrangian Eulerian) formulation and FSI (Fluid-Structure Interaction) analysis technique of LS-DYNA code through the verifications of internal blast tests of reduced scale and partial chamber models.

Keyword Words: *Internal Blast, Blast Hardened Bulkhead (BHB), Reduced Scale and Partial Chamber Models, MMALE (Multi-Material Arbitrary Lagrangian Eulerian), Fluid-Structure Interaction (FSI) Analysis Technique, LS-DYNA code*

2 Introduction

It is necessary to restrict the damage area for the enhancement of ship survivability under the internal blast of Semi-Armor Piercing (SAP) warhead inside the compartment of naval ship, as shown in Fig. 1, and to develop design guidance and performance verification technique of Blast Hardened Bulkhead (BHB) for the protection of its damage diffusion to adjoining compartments and continuous flooding. BHB was already developed and has been applied to the naval ship in some countries [1, 2], and has been partially adopted to some navy ships with the foreign techniques.

Diverse scale internal blast tests of BHB were carried out, and its design and analysis techniques were also verified for its application abroad. TNO carried out full scale internal blast test of BHB through the internal blast test using retired naval ship [1], as shown in Fig. 2, and DSTO, also, internal blast test of part transverse bulkhead model of real one, as shown in Fig. 3(a), and investigated its shock response and factors related to the design constraints [3]. Diverse scale internal blast tests were performed using real scale compartment of naval ship, etc., as shown in Fig. 3(b), in the USA.



Fig. 1: Internal explosion damage of USS Stark (FFG-31) by Exocet Missiles [3]



Fig. 2: Internal blast test of retired ship and BHD model by TNO [1]



(a) partial model by DSTO [3] (b) real scale in USA
Fig. 3: Internal blast test of partial and full scale bulkhead model

For the self-development of BHB, its effective analysis, design and verification techniques are needed based on the full scale internal blast test. Structural behavior evaluation technique under the internal blast is necessary to reduce the cost and time for the BHB design, and to estimate the exact response behavior according to design pattern and size, through the prediction of diverse behaviors according to the BHB design by the numerical simulation instead of explosion test. MMALE (Multi-Material Arbitrary Lagrangian Eulerian) formulation and FSI (Fluid-Structure Interaction) analysis technique of LS-DYNA code [4] were used for the development of shock response analysis technique of BHB under the internal blast.

In this study shock response analysis of 5 bulkhead models was carried out for the internal blast test of reduced scale chamber as the basis research for the real scale blast test, structural behavior analysis technique was verified, and their shock response characteristics was also figured out. At the next step, response analysis of real scale partial chamber model with 2 bulkhead models and several stand-off distances was performed and compared with test results for the internal blast test based on the reduced scale chamber test and response analysis results.

3 Internal Blast Test of Reduced Scale and Partial Chamber Models

Reduced scale and partial chamber models are largely consisted of chamber, bulkhead structure and clamp frame, as shown in Figs. 4 & 5, with the ratio of chamber dimension as 2:1:0.75 by its length, breadth and height, and the dimension ratio of reduced scale and partial ones as 1: 0.25. Detachable bulkhead structure was replaced in every test, and was compressed by the wedges between cartridge and clamp frames for the protection of explosion shock pressure leakage between chamber and bulkhead cartridge. Measuring gauges were attached on the bulkhead and measured for the pressure, acceleration and strain responses under the internal blast test, as shown in Figs. 4(b) & 5(b).



(a) front view without bulkhead (b) front view with bulkhead (c) rear view with opening (d) iso view of chamber test model
Fig. 4: Reduced scale chamber model for internal blast test



(a) front view without bulkhead (b) front view with bulkhead (c) rear view with opening (d) iso view of chamber test model
Fig. 5: Partial chamber model for internal blast test

In reduced scale chamber test model, bulkhead plate and stiffeners were welded to the inserted plate, as shown in Fig. 6(a) & (b), and the whole inserted plate was contacted to the inside of cartridge frame and attached by spot welding along its center line, as shown in Fig. 6(c). Cartridge frame was manufactured by welding two SQ pipes partially. In partial chamber, bulkhead was installed inside the SQ pipe type cartridge with three stiffeners. Mild steel (SS41) was used for whole parts of two types of chamber models, except the bulkhead and stiffeners of partial chamber with high tensile steel (AH36).



(a) front side (b) back side (c) spot welding in inserted plate
Fig. 6: Reduced scale bulkhead model

Table 1 summarizes the general information of 5 bulkhead models, such as curtain and plain bulkhead plate type, the number of side welding edge of bulkhead and inserted plate, the number of basic and auxiliary stiffeners, welding type between sponson part of inserted plate and cartridge frame. Figure 7 shows the schematic diagram of bulkhead according to the number of side welding edge. Bulkhead models 1~3 were used for the first internal blast test, and bulkhead models 4~5, for the second one. High explosive (HE) and low explosive (LE) TNT charges were used for each chamber model, where the ratio of HE and LE TNT charge was 1: 0.075.

Table 1: Information of 5 bulkhead models of reduced scale chamber model

model	plate type	No. of side welding edge	No. of BH stiffeners	welding type bt. inserted plate & cartridge
1	curtain	4	3	partial
2	plain	4	3	partial
3	plain	3	3+1(auxiliary)	partial
4	plain	4	3+2(auxiliary)	continuous
5	plain	2	4	continuous

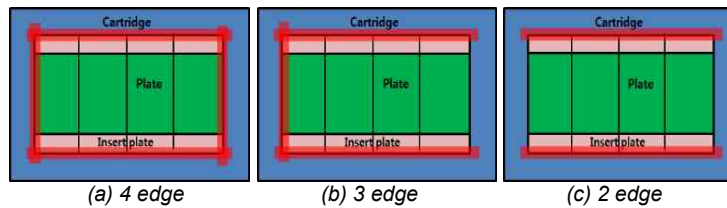


Fig. 7: Schematic diagram of bulkhead according to welding edge

Two types of bulkheads, such as plain and curtain types, were considered for the internal blast test of partial chamber model, as shown in Table 2. The ratio of HE and LE TNT charges was also 1: 0.075, as the reduced scale chamber model, however, their TNT charge ratio was 1: 0.0156. Internal blast test and shock response results of HE and LE TNT charges were considered and compared with each other. Three stand-off distances, such as 1/2L, 1/4L and 1/8L, were typically considered for the shock response characteristics and plastic deformation of plain plate type bulkhead, where L stands for the chamber length. Curtain plate type bulkhead was also considered at stand-off distance 1/2L together with reversed direction of bulkhead, as shown in Table 2. The last test was the close internal blast one for the fracture criterion of bulkhead material and welding effect with double HE TNT charge.

Table 2: Information of 2 bulkhead models of partial chamber model

Model	Bulkhead type	Location of explosive	Type of explosive	Direction of bulkhead	No. of test
1	plain	1/2L	HE TNT	normal	3 & 6
2	plain	1/4L	HE TNT	normal	4
3	plain	1/8L	HE TNT	normal	2
4	plain	1/2L	LE TNT	normal	1 & 5
5	curtain	1/2L	HE TNT	normal	9
6	curtain	1/2L	HE TNT	reversed	10
7	plain	1/16L	2 x HE TNT	normal	11

Damage configurations of 5 reduced scale chamber bulkhead models are shown in Fig. 8 under internal blast test. It could be found that damage response of bulkhead structure with relatively thin plate, 2.0mm, was very sensitive to the welding effect. These characteristics were suitably realized by modeling for the internal blast response analysis. As the bulkhead was bent outward, outside inserted plate contacted to the cartridge was also bent outward and was integrated to the cartridge. Since the sponson part of inside inserted plate was also bent inward, its sponson part was detached or attached according to their partial and continuous welding condition to the cartridge.



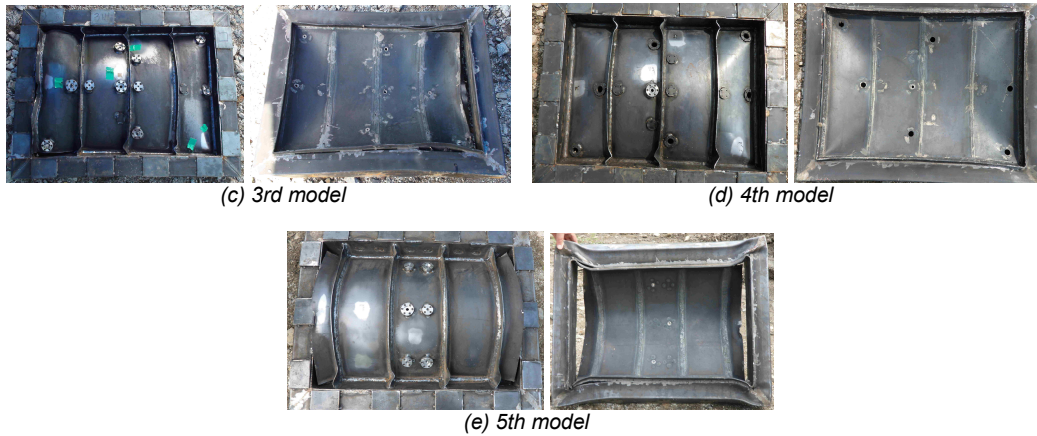


Fig. 8: Damage configurations of reduced scale chamber bulkhead models under internal blast test

Figure 9(a) & (b) shows the damaged configuration of plain type bulkhead and curtain type one with reversed direction at stand-off distance $1/2L$, respectively. The every end of stiffeners was only torn away in the curtain plate type bulkhead with reversed direction in this blast test of partial chamber model. The fracture at the end of stiffener occurred at the location off the welding bead, not at the welding line. The bead thickness was considered in the shock response analysis. For the establishment of fracture criterion in partial chamber bulkhead model, very close internal blast test was carried out, where the whole bulkhead was torn away from the bulkhead bead attached in cartridge and most upper and bottom cartridge part, also, along the bulkhead welding line, as shown in Fig. 10.



Fig. 9: Damage configuration of partial chamber bulkhead under internal blast test at $1/2L$ stand-off distance

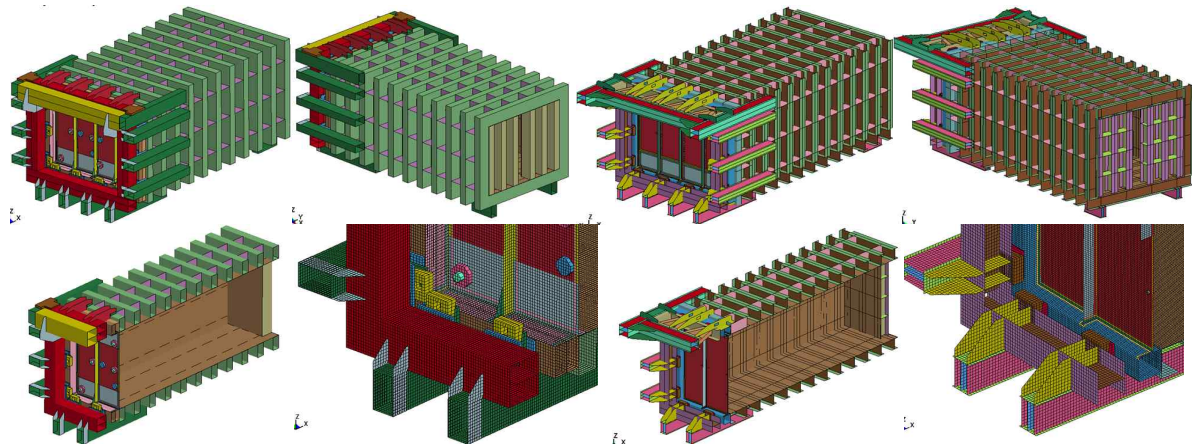


Fig. 10: Damage configurations of partial chamber bulkhead under internal blast test with 2xHE TNT at $1/16L$ stand-off distance

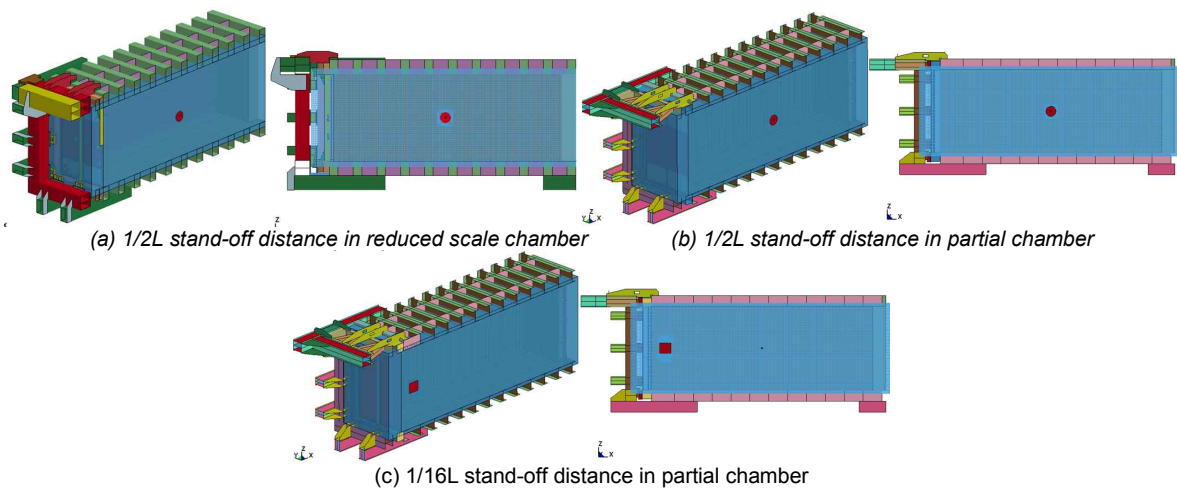
4 Modeling of Shock Response Analysis of Chamber Models

Shock response analyses were carried out for reduced scale and partial chamber model by the schedule, as shown in Tables 1 & 2, and their F.E. configurations are shown in Fig. 11. Figure 12

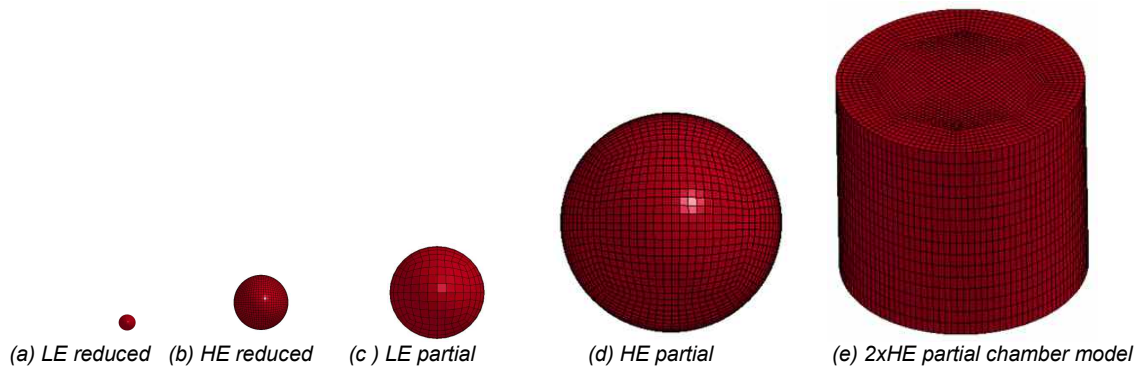
shows the F.E. configuration of air, TNT charge and chamber model according to stand-off distance of TNT charge. Typical TNT charges are shown in Fig. 13, such as spherical type LE & HE in reduced scale chamber model, spherical type LE & HE in partial one, and cylindrical type 2xHE in partial one. Figure 14 illustrates the modeling of bulkhead in reduced scale and partial chamber, and Fig. 15(a)~(f), 5 bulkhead models of reduced scale chamber. Figure 15(g)~(h) shows the close view of partial chamber bulkhead model, and Fig. 15(i)~(j), additional welding and concrete ones for the internal blast of 2xHE TNT charge at stand-off distance 1/16L. MAT_CSCM_CONCRETE option was used for the concrete damage shock response. Shell and solid elements were used for their structures and MMALE of air and charge, respectively, with around 476,000 shell and 2,700,000 solid element numbers for reduced scale chamber model and around 515,000 shell and 8,520,000 solid ones for partial chamber one.



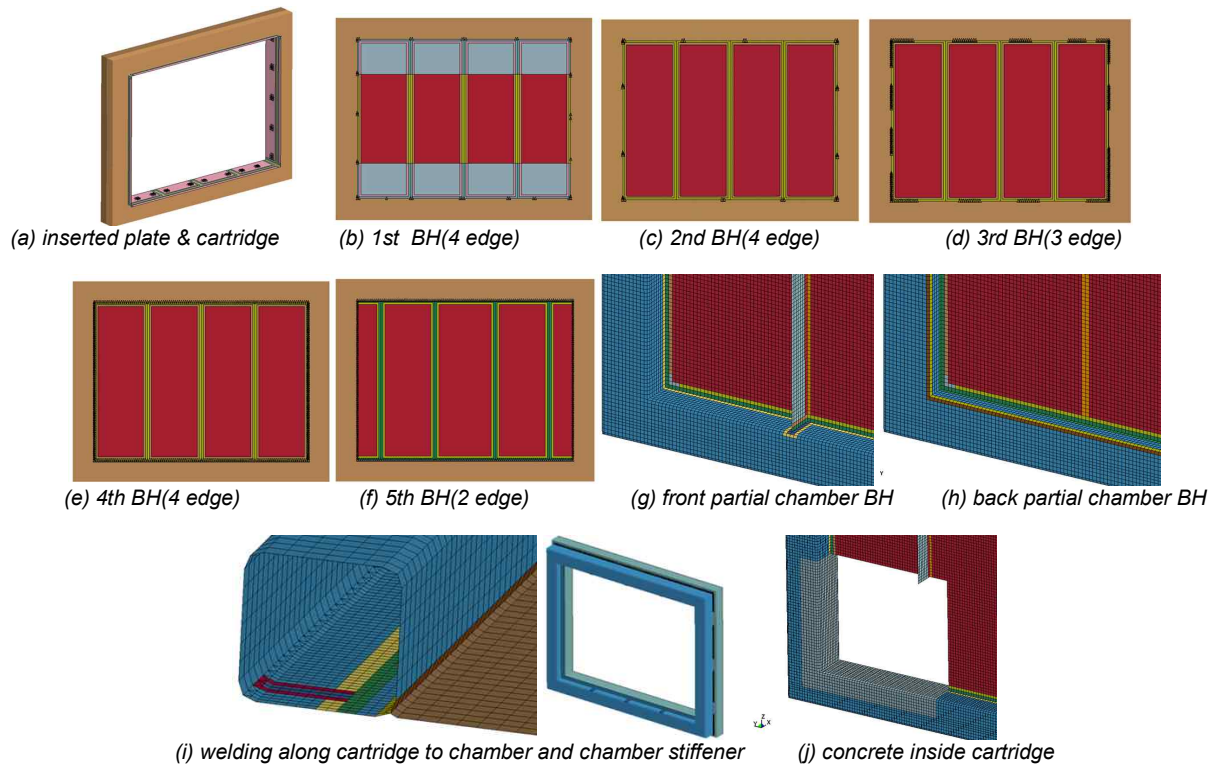
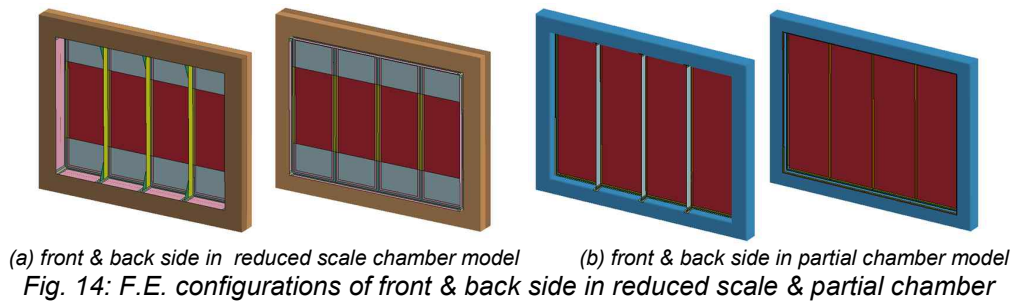
(a) reduced scale chamber model (b) partial chamber model
 Fig. 11: F.E. configurations of reduced scale and partial chamber models



(a) 1/2L stand-off distance in reduced scale chamber (b) 1/2L stand-off distance in partial chamber
 (c) 1/16L stand-off distance in partial chamber
 Fig. 12: F.E. configurations of air, HE TNT charge and reduced scale & partial chamber models



(a) LE reduced (b) HE reduced (c) LE partial (d) HE partial (e) 2xHE partial chamber model
 Fig. 13: F.E. configurations of TNT charge according to HE & LE, reduced scale & partial chamber, 2xHE in partial chamber

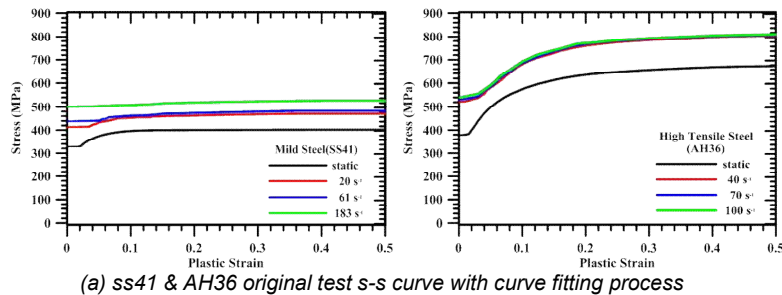


Inserted plate was contacted to the inside of chamber using CONTACT_SURFACE_TO_SURFACE option, and was welded along the centerline to the cartridge using CONSTRAINED_NODE_SET option, as shown in Fig. 15(a). Partial and continuous welding of the sponson part of inserted plate to the cartridge in reduced scale chamber model was treated by CONSTRAINT_SPOTWELD option, as shown in Fig. 15(b)~(f). Welding effect was treated by increasing the thickness of the welding bead, and by decreasing the failure strain in the neighboring strip near the bead, as shown in Fig. 15(g)~(h). In reduced scale chamber bulkhead, bulkhead was torn away along the bead, since the bulkhead was very thin. Welding line of bulkhead was treated by controlling the failure strain with consideration of the bead thickness. Wedge was pre-stressed and was stuck to the chamber, as shown in Fig. 11. Air ALE solid element was modeled for the surround of the chamber and bulkhead structures, and FSI analysis technique was applied to the air and charge MMALE and chamber and bulkhead structure using CONSTRAINED_LAGRANGE_IN_SOLID option of LS-DYNA code.

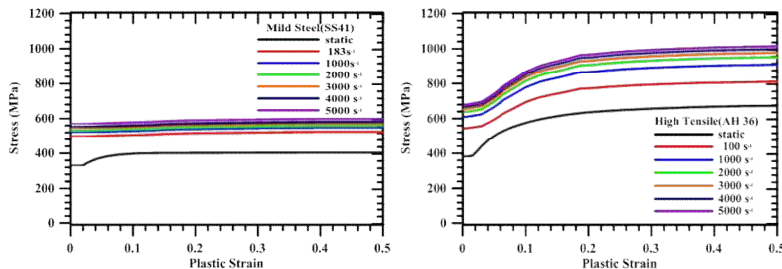
Some stress-strain curves of mild steel (SS41) and high tensile steel (AH36) with short strain range were obtained by the static and high speed tensile test, and curve fitting process was applied to the original ones, as shown in Fig. 16(a). Extended stress-strain curves were suggested for the high strain rate in the case of close internal blast, such as stand-off distance $1/16L$ and $2xHE$ TNT charge, using Cowper-Symonds equation, as shown in Fig. 16(b). Their general properties are summarized in Table 3. Shear strain fracture model was adopted for the fracture of structure in the shock response analysis and failure strain was applied to the chamber structure according to the element size to its thickness and welding effect. MAT_PIECEWISE_LINEAR_PLASTICITY(MAT_024) was adopted for the mild and high tensile steels. Pressure and acceleration responses were measured at the locations on reduced scale and partial chamber bulkheads, as shown in Fig. 17.

Table 3: Properties of mild and high tensile steels

Property	Mild steel(SS41)	High tensile steel(AH36)
Young's modulus	206 GPa	206 Gpa
Density	7,850 kg/m ³	7,850 kg/m ³
Poisson's ratio	0.3	0.3
Mild stress	330 MPa	405 MPa
Ultimate stress	380 MPa	676 MPa
Failure strain	0.10 ~ 0.60	0.10 ~ 0.60

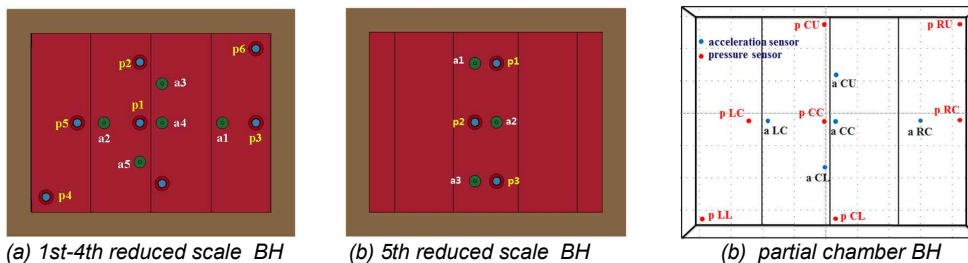


(a) ss41 & AH36 original test s-s curve with curve fitting process



(b) ss41 & AH36 extended s-s curve using Cowper & Symond model

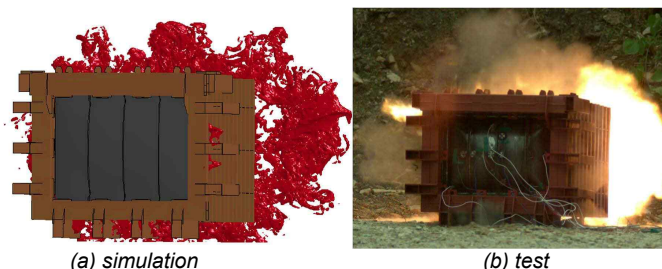
Fig. 16: Stress-strain curves of mild and high tensile steels with strain rate effect



(a) 1st-4th reduced scale BH (b) 5th reduced scale BH (c) partial chamber BH
Fig. 17: Pressure & acceleration sensor locations on reduced scale & partial chamber bulkheads

5 Shock Response Analysis of Chamber Models

Figure 18 shows the blast flame configuration from the backward opening and side leakage between chamber and bulkhead cartridge in the case of simulation and test of reduced scale chamber model under the internal blast of HE TNT charge, and Fig. 19 shows the propagation process of shock wave at the longitudinal vertical plane in the partial chamber model according to the stand-off distance of HE TNT charge under internal blast. The difference of shock wave propagation to the bulkhead could be figured out well between initial shock wave and reflect wave against the internal chamber wall according to the location of HE TNT charges.



(a) simulation (b) test
Fig. 18: Blast frame in reduced scale chamber model under internal blast of HE TNT charge

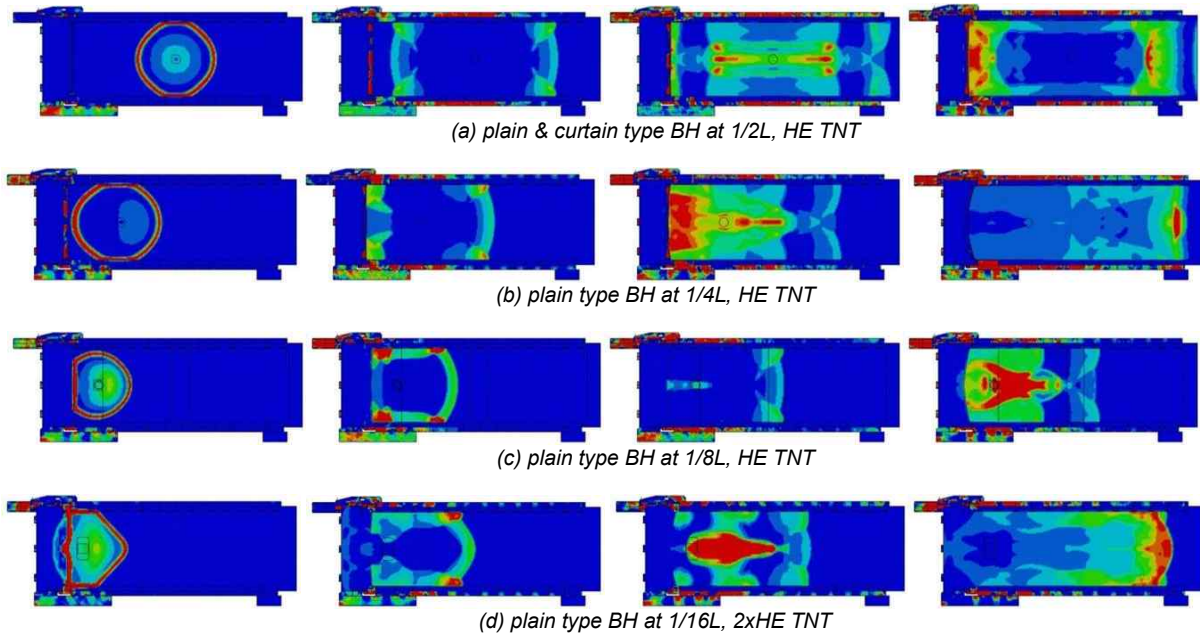


Fig. 19: Propagation of shock pressure in part chamber model according to stand-off distance of HE TNT charge

Figure 20 shows the overall maximum stress, plastic strain and deformation response configurations of reduced scale chamber including curtain type bulkhead with HE TNT charge, and Fig. 21, the overall maximum plastic strain distributions of partial chamber including curtain and plain type bulkheads according to stand-off distance with HE TNT charge. Very large responses could be found at the bulkhead compared to the chamber and clamp frames.

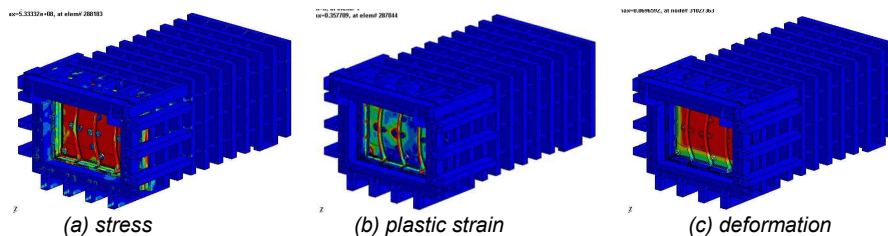


Fig. 20: Damage response configurations of reduced scale chamber model with HE TNT charge

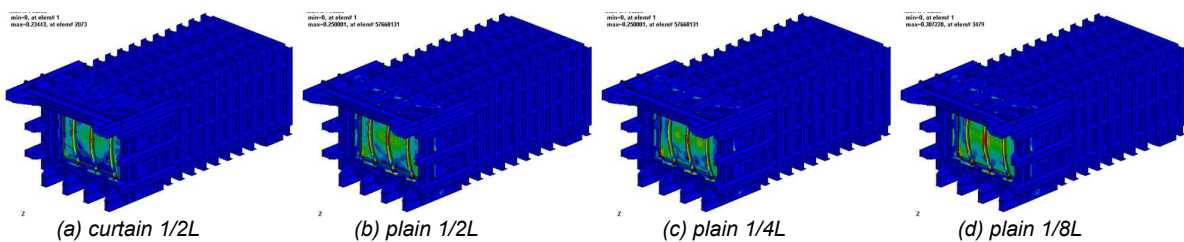


Fig. 21: Plastic strain response configurations of partial chamber model according to stand-off distance of HE TNT charge

Figure 22 shows the damage response configurations in reduced scale chamber bulkhead models, such as plastic strain, under the internal blast simulations of HE TNT charge. From these damage responses, very sharp stress concentration parts and rupture configurations could be found in the bulkhead, stiffeners and cartridge frame, and damage responses, also confirmed to be very sensitive to the welding condition due to the very thin bulkhead plate as shown in the internal blast test results of Fig. 8. The mechanism of the inserted plate to the cartridge could be also found to play a decisive role in deformation and damage in reduced scale chamber bulkhead according to the welding range to the cartridge in the internal blast test and simulation. It could be found that damage configuration of each bulkhead generally shows good agreement with internal blast test result of Fig. 8.

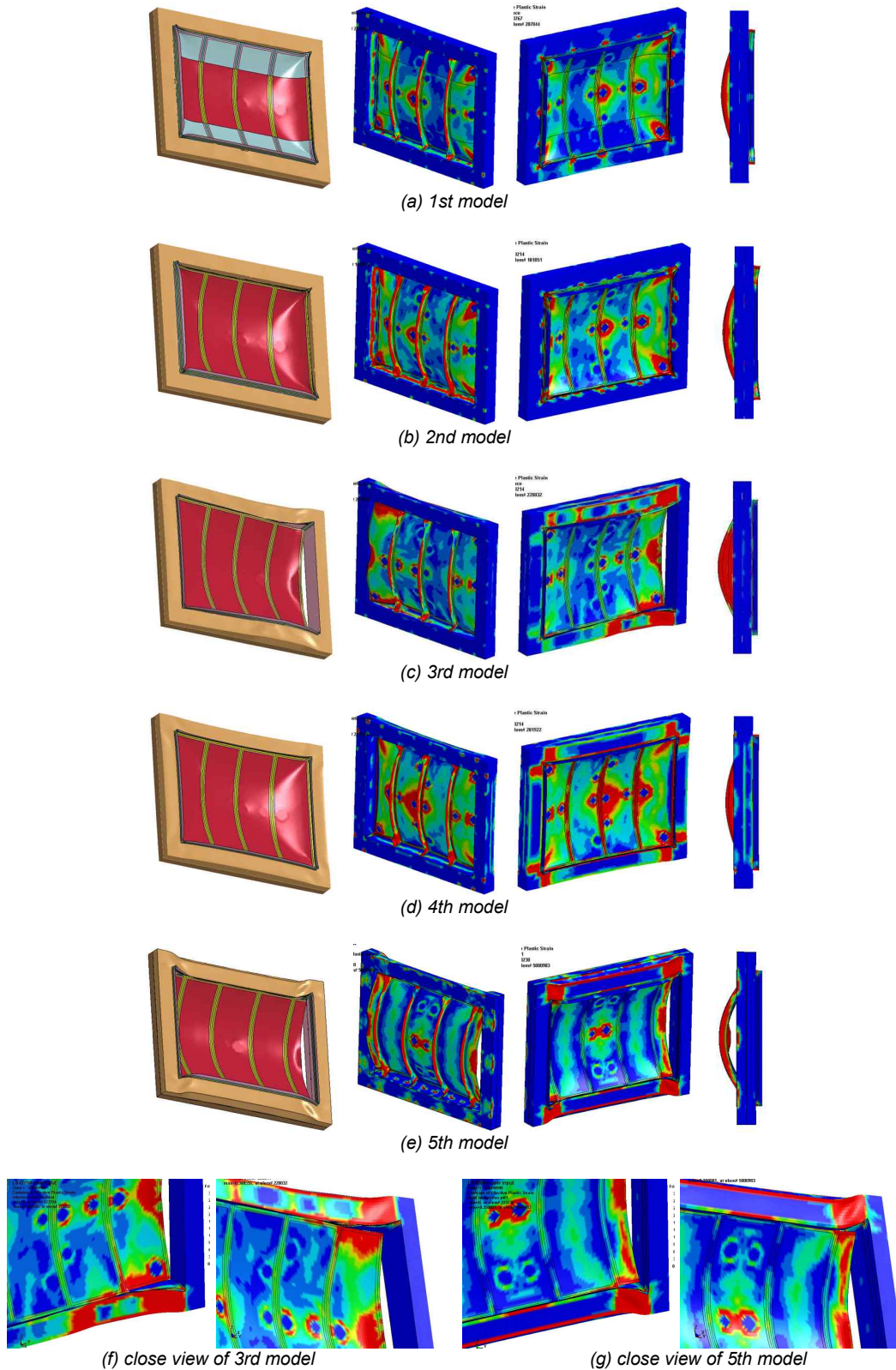
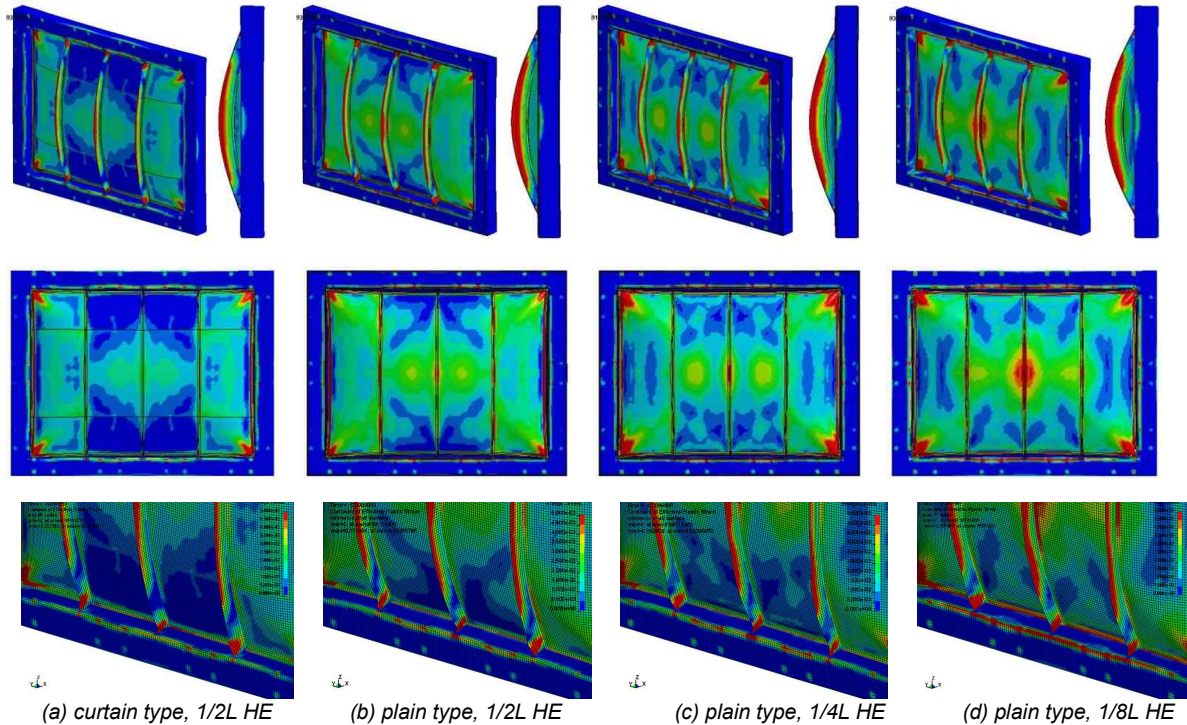


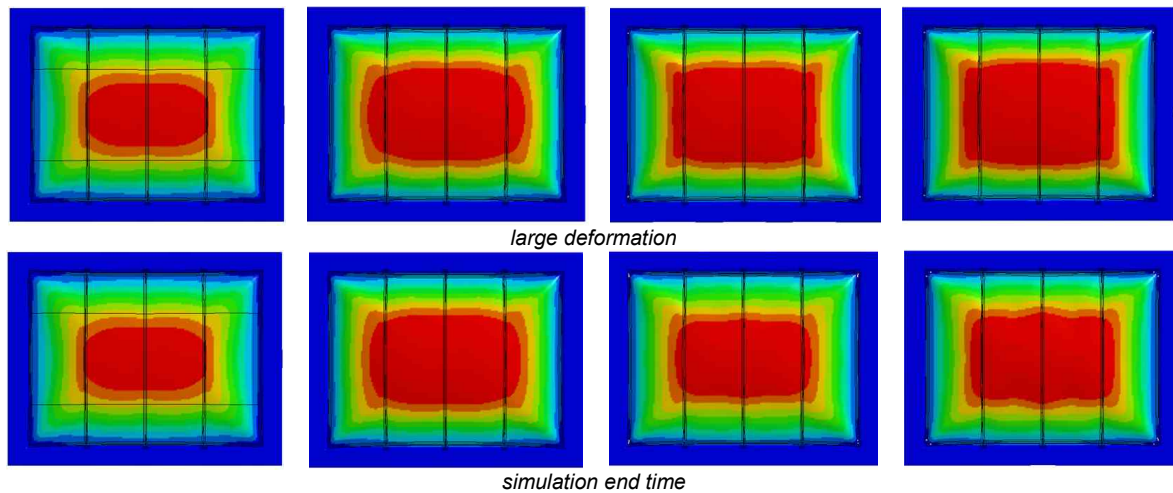
Fig. 22: Damage response configurations in reduced scale chamber bulkhead models under internal blast simulation of HE TNT charge

Figures 23 & 24 illustrate the plastic strain and deformation response configurations at the partial chamber curtain and plain type bulkheads according to the stand-off distance HE TNT charge, respectively, and Figs. 25 & 26, their plastic strain responses at the center, corners of bulkhead and the end of stiffeners, and deformation responses along the vertical, horizontal and diagonal directions

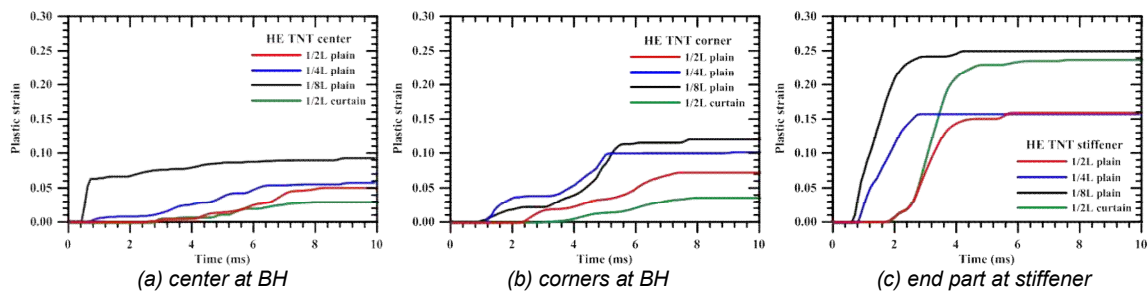
from the center at the bulkhead for the confirmation of their response according to bulkhead type and stand-off distance HE TNT charge, respectively.



(a) curtain type, 1/2L HE (b) plain type, 1/2L HE (c) plain type, 1/4L HE (d) plain type, 1/8L HE
 Fig. 23: Plastic strain response configurations in curtain and partial type bulkheads according to stand-off distance of HE TNT charge



(a) curtain type, 1/2L HE (b) plain type, 1/2L HE (c) plain type, 1/4L HE (d) plain type, 1/8L HE
 Fig. 24: Deformation response configurations in curtain and partial type bulkheads according to stand-off distance of HE TNT charge



(a) center at BH (b) corners at BH (c) end part at stiffener
 Fig. 25: Plastic strain responses in curtain and partial type bulkheads according to stand-off distance of HE TNT charge

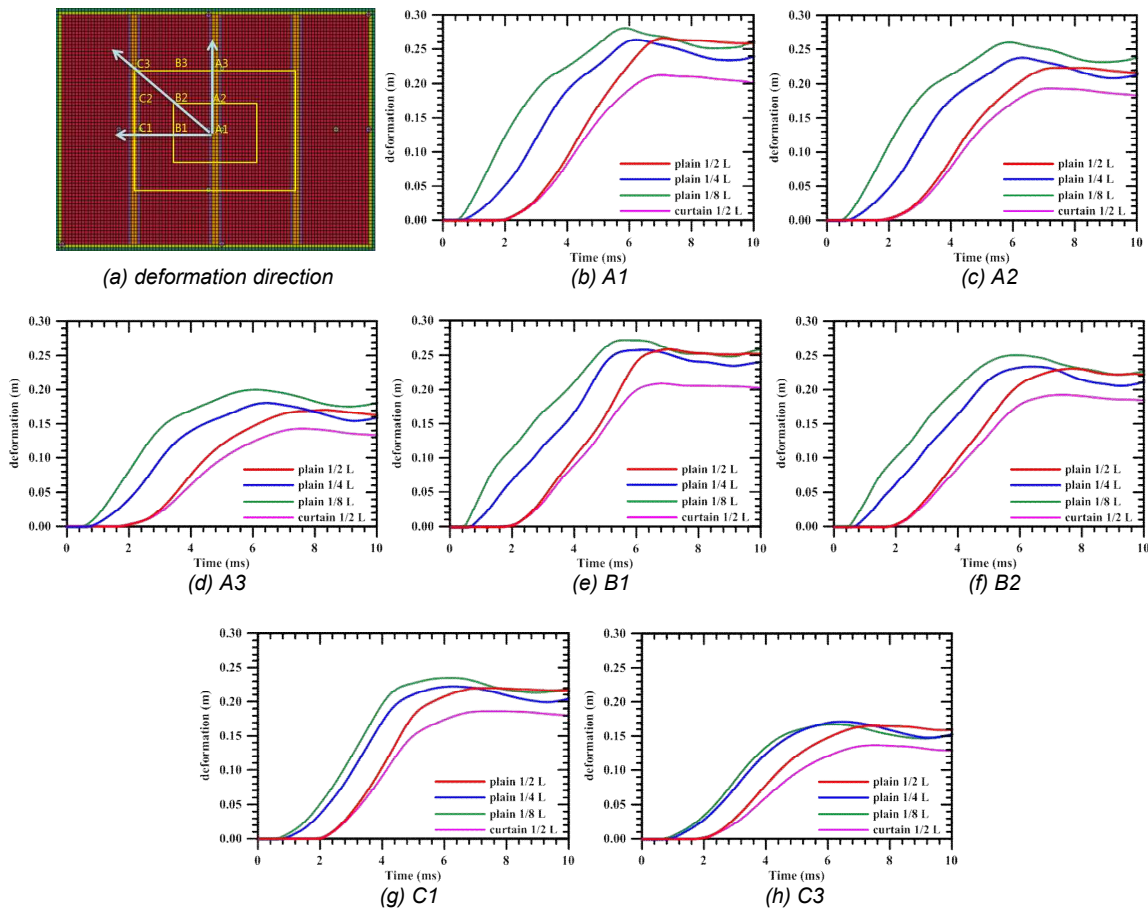


Fig. 26: Deformation responses in curtain and partial type bulkheads according to stand-off distance of HE TNT charge

As expected, the maximum and range of plastic strain of the plain type bulkhead increased at the center of bulkhead with the decrease of stand-off distance of HE TNT charge to the bulkhead, and large plastic strain also occurred at the corners of bulkhead with the decrease of stand-off distance of HE TNT charge to the bulkhead, since the shock pressure was impacted to the corners by the reflection wave. Those of the curtain type bulkhead occurred relatively smaller than those of the plain type bulkhead at stand-off distance 1/2L of HE TNT charge. Very high plastic strain also occurred at the end of stiffeners next to the welding bead together with buckling phenomena because of compression, and the same trends appeared as the center and corners of bulkhead according to stand-off distance of HE TNT charge and bulkhead type. However, there was no rupture in every bulkhead including stiffeners in the bulkhead type and stand-off distance of HE TNT charge. The plain type bulkhead generally deformed larger and more widely compared to the curtain type one. Unexpectedly, deformation magnitude and range at the plain type bulkhead were not increased linearly according to the decrease of stand-off distance of HE TNT charge to the bulkhead, and they were decreased and increased again as the stand-off distance of HE TNT charge from 1/2L, 1/4L and 1/8L, as shown in Figs. 24 & 26, which might be due to the reflection wave to the corners.

In the case of the curtain type bulkhead with reversed direction at the stand-off distance 1/2L of HE TNT charge, stiffeners buckled and their only end parts were torn away in the neighbor layer near welding bead in the internal blast simulation and test, as shown in Figs. 9(b) & 27. Very close internal blast simulation results are shown in Fig. 28, and the whole bulkhead was torn away from the bulkhead bead attached in cartridge and most upper and bottom cartridge part, also, along the bulkhead welding line with broken concrete, as shown in Fig. 10. Very huge velocities could be found at the center, mid points of upper and side at bulkhead in the internal blast simulation, as shown in Fig. 28. Fracture criterion could be set up for this internal blast simulation considering welding effects.

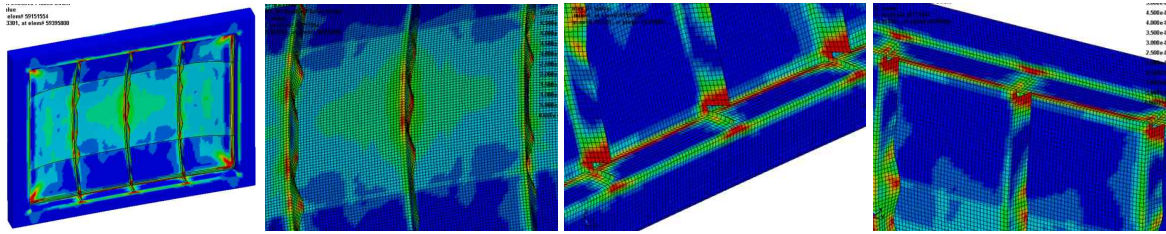


Fig. 27: Damage configurations of curtain type bulkhead under HE TNT charge with reversed direction and stand-off distance 1/2L

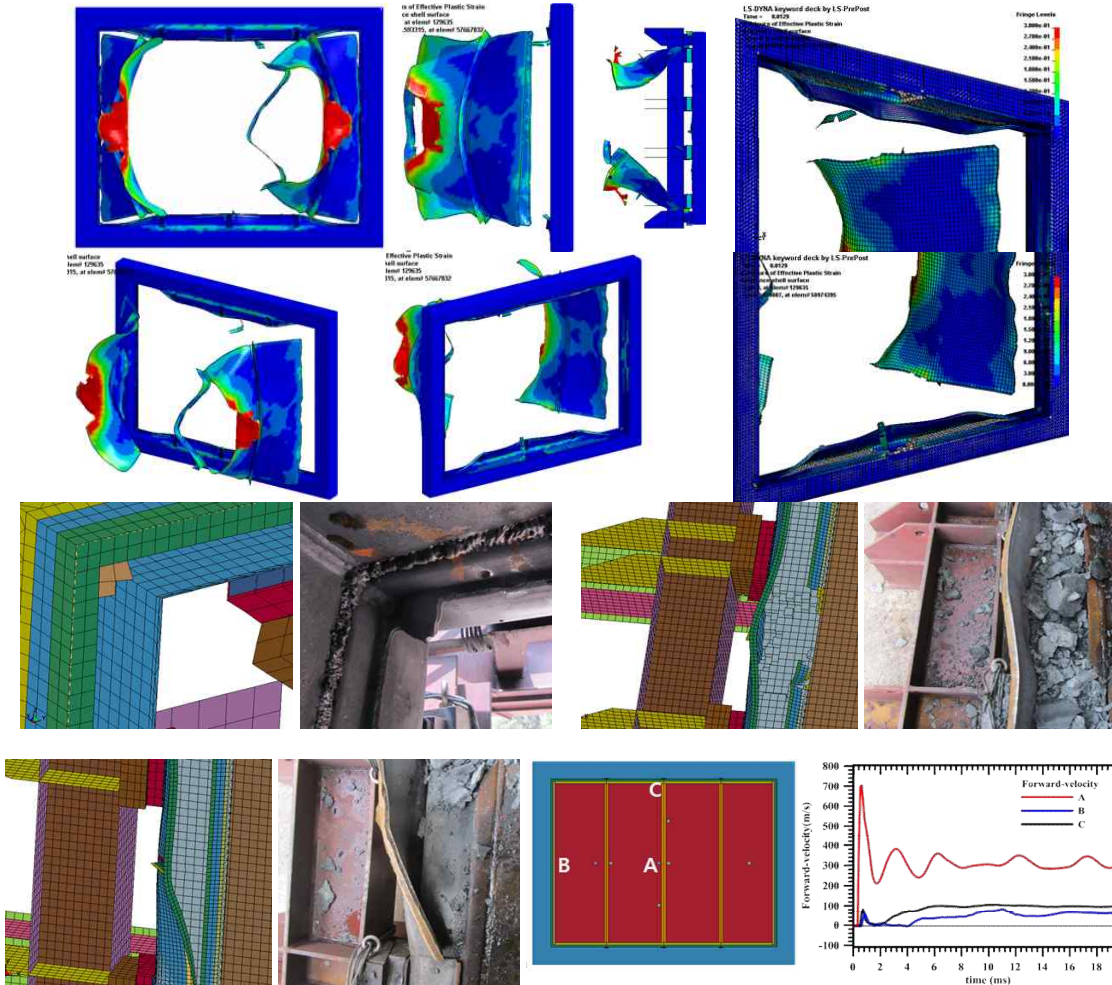
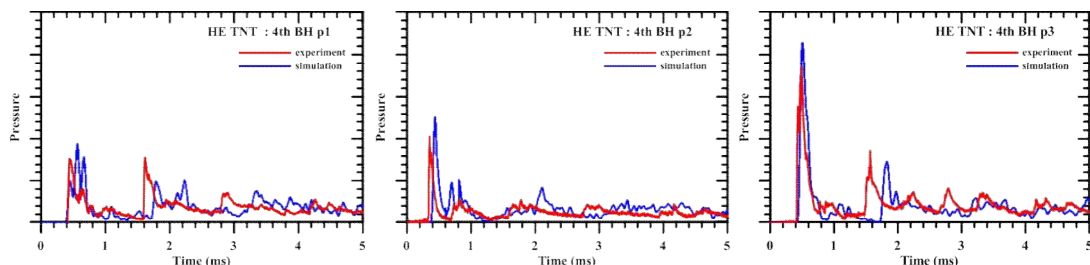


Fig. 28: Damage configurations of plain type bulkhead under 2xHE TNT charge at and stand-off distance 1/16L

Responses could not be measured fully correctly in the first internal blast test using the 1st~3rd reduced scale chamber models, with only some pressure ones of the 2nd one. Both pressure and acceleration responses of the 4th and 5th models were measured at the locations of bulkhead, as shown in Fig. 17(a)~(b), and compared to those of test with HE TNT charge, as shown in Figs. 29~32, respectively. All responses are represented by the non-dimensional scale. It could be found that the pressure and acceleration responses generally show good agreement with those of internal blast test.



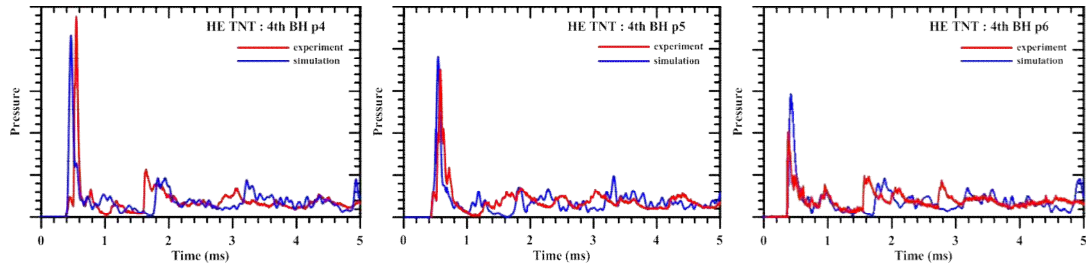


Fig. 29: Pressure responses between experiment & simulation with HE TNT at 4th bulkhead

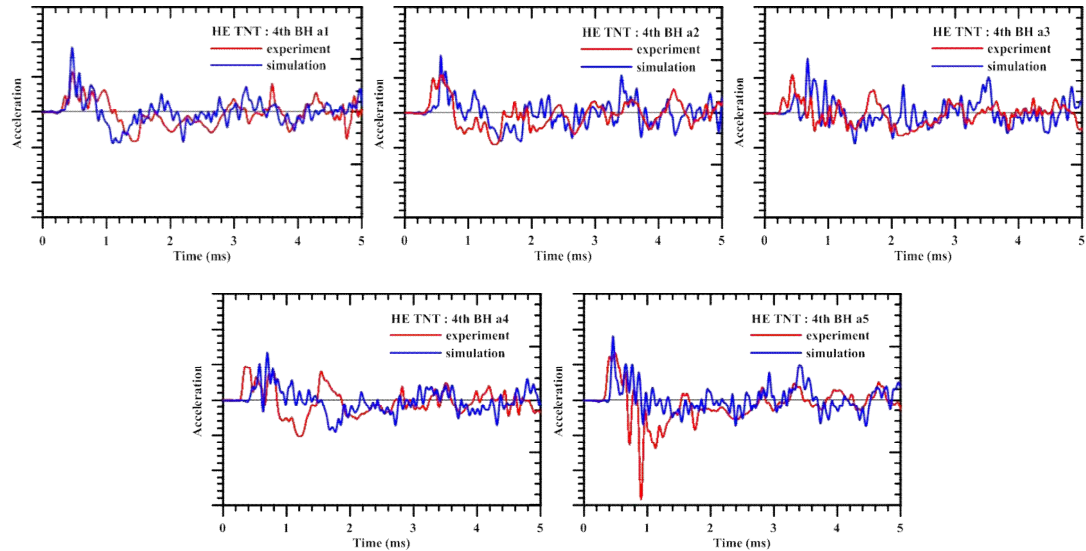


Fig. 30: Acceleration responses between experiment & simulation with HE TNT at 4th bulkhead

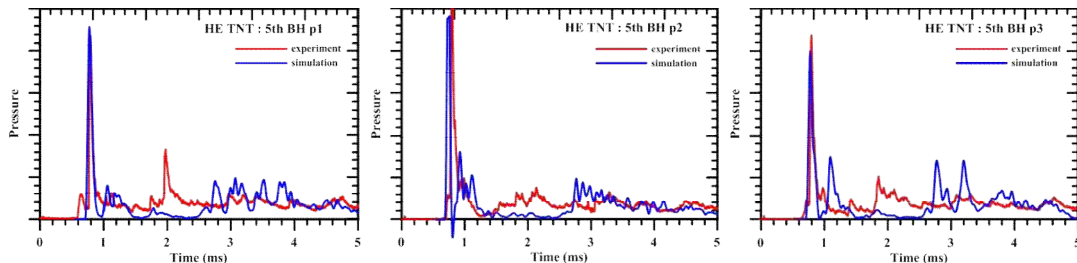


Fig. 31: Pressure responses between experiment & simulation with HE TNT at 5th bulkhead

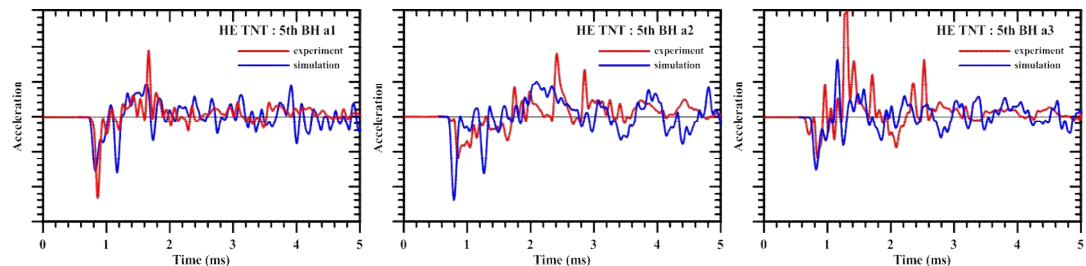


Fig. 32: Acceleration responses between experiment & simulation with HE TNT at 5th bulkhead

Pressure and acceleration responses were measured at the locations of bulkhead, as shown in Fig. 17(c). Among the whole internal blast test of partial chamber models, pressure and acceleration responses of plain type bulkhead at stand-off distance $1/2L$ & $1/4L$ and curtain one at stand-off distance $1/2L$ were typically compared to those of internal blast tests, as shown in Fig. 33~38. It could be also found that the pressure and acceleration responses generally show good agreement with those of internal blast test, as the case of reduced scale chamber models.

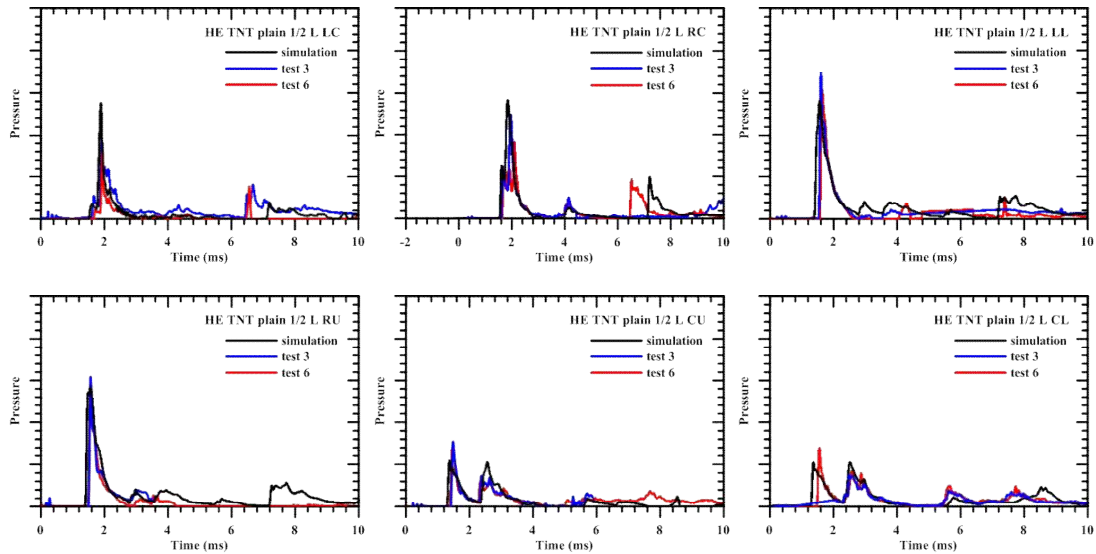


Fig. 33: Pressure responses between experiment & simulation with HE TNT in plain type bulkhead at stand-off distance 1/2L

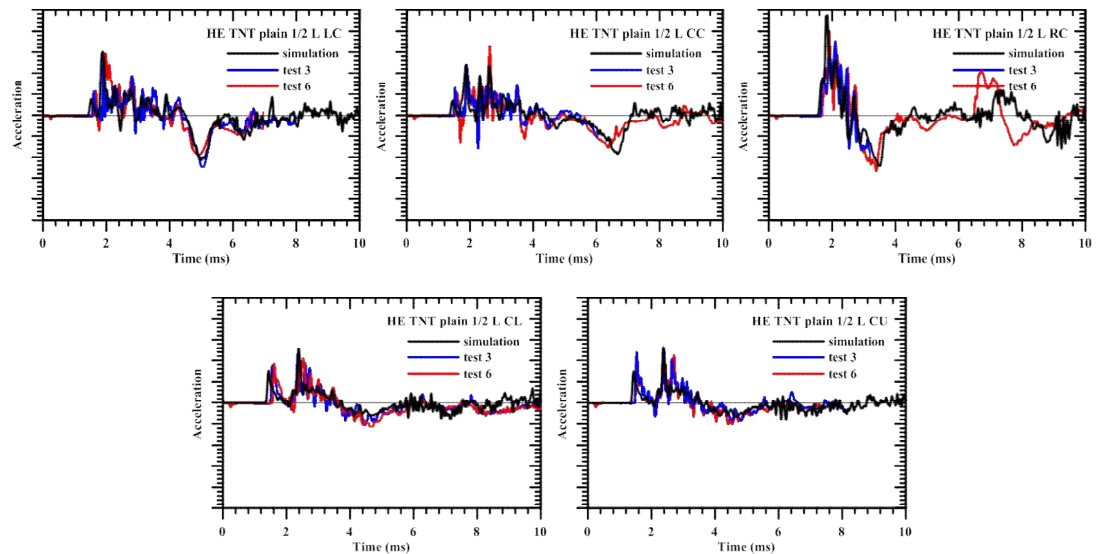


Fig. 34: Acceleration responses between experiment & simulation with HE TNT in plain type bulkhead at stand-off distance 1/2L

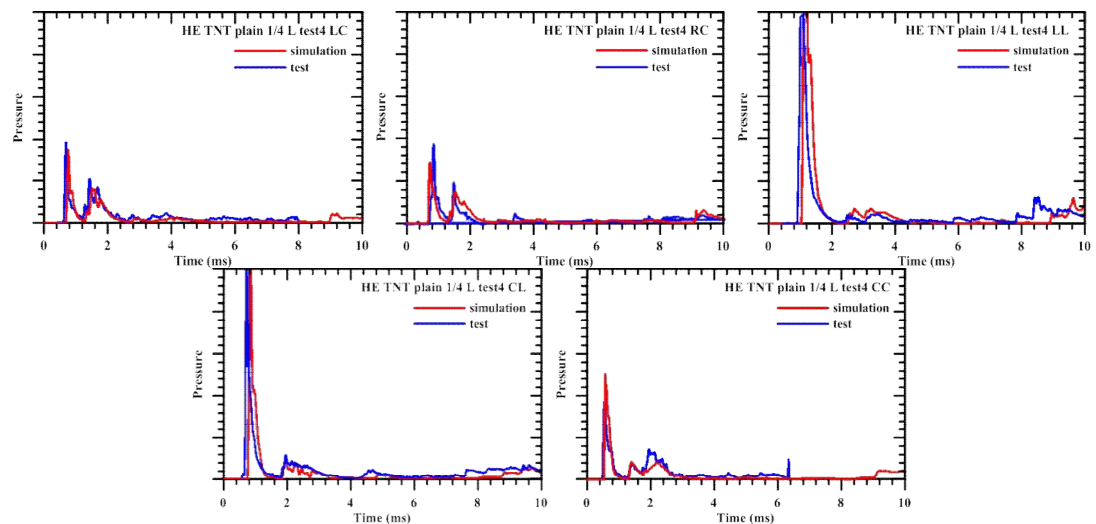


Fig. 35: Pressure responses between experiment & simulation with HE TNT in plain type bulkhead at stand-off distance 1/4L

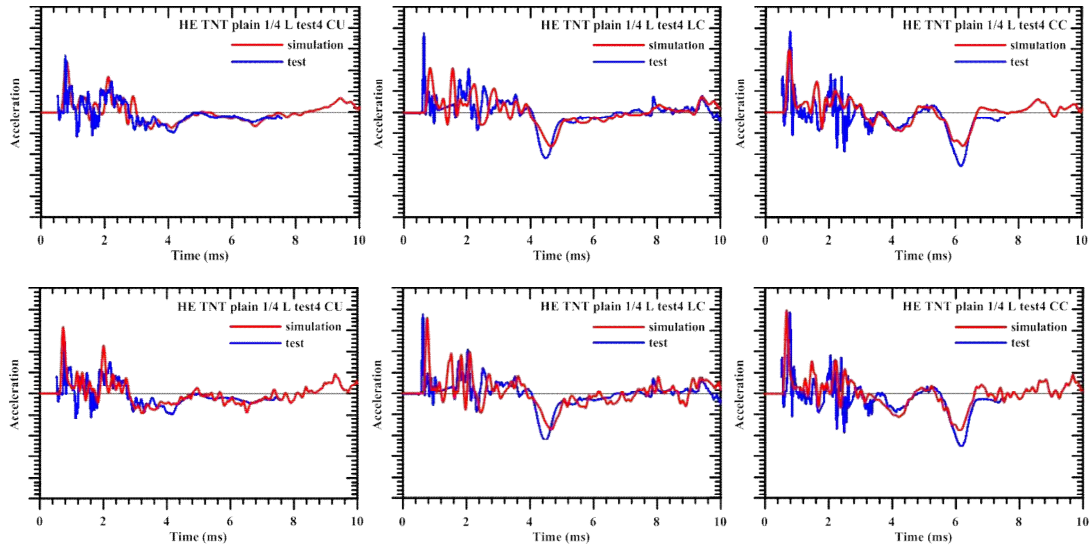


Fig. 36: Acceleration responses between experiment & simulation with HE TNT in plain type bulkhead at stand-off distance 1/4L

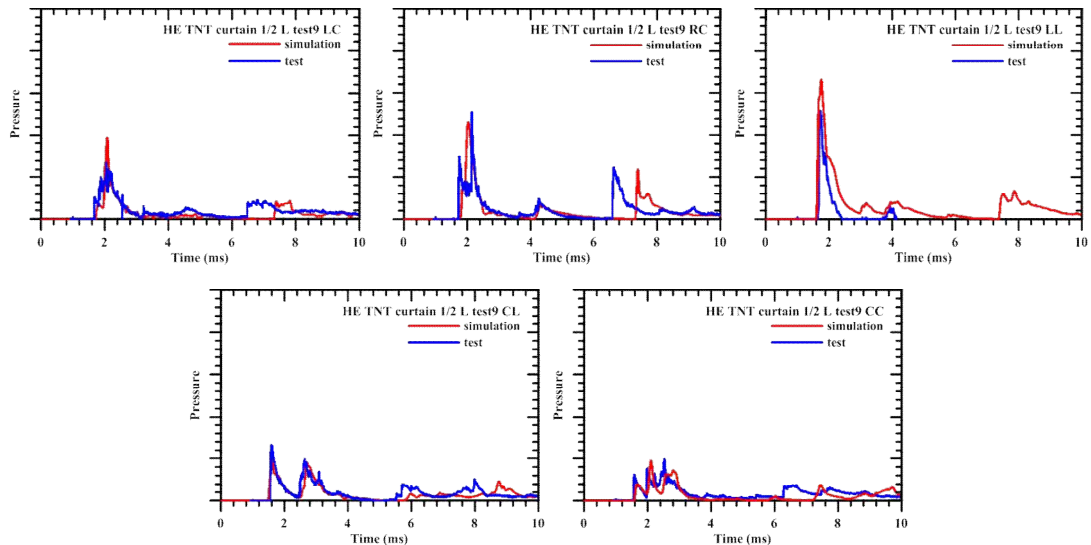


Fig. 37: Pressure responses between experiment & simulation with HE TNT in curtain type bulkhead at stand-off distance 1/2L

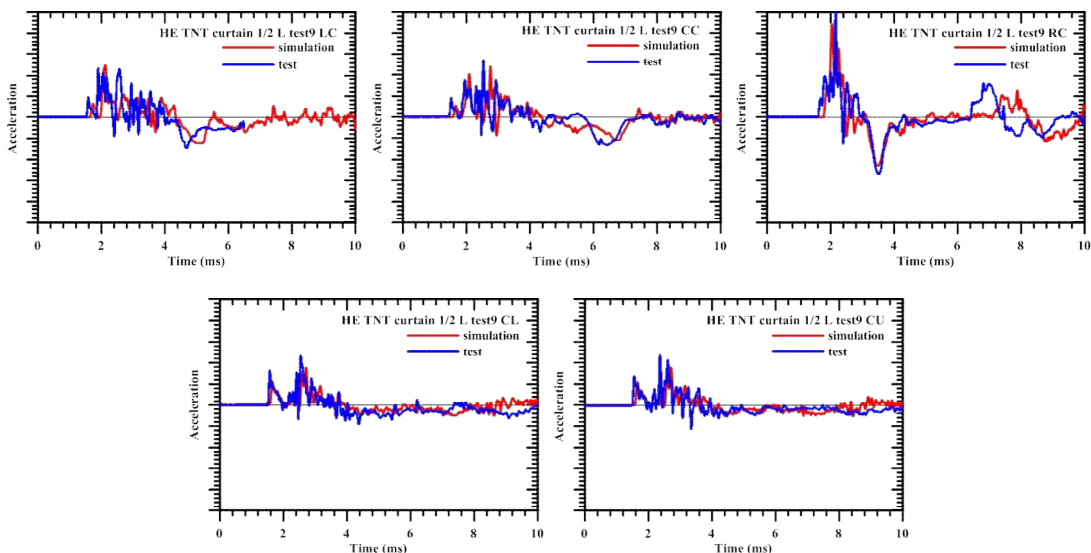


Fig. 38: Acceleration responses between experiment & simulation with HE TNT in plain type bulkhead at stand-off distance 1/2L

6 Summary

In this study, shock response analysis was carried out for the reduced scale and partial chamber models under the internal blast, and its response analysis technique was verified with the test results of 5 bulkhead models of reduced scale chamber models and 2 types of bulkheads of partial chamber ones according to stand-off distance of HE and LE TNT charges, using MMALE formulation and FSI analysis technique of LS-DYNA code. Shock response characteristics could be also figured out through the verifications of response analysis technique compared with the internal blast test results.

Through the verifications of the internal blast simulations with test results, important factors should be considered carefully, such as FSI analysis techniques, damage mechanism, fracture criterion, and welding effects. It could be found that damage configurations of each bulkhead generally showed good agreement with those of internal blast tests, and that pressure and acceleration responses of shock response analysis, also with those of tests.

7 Acknowledgement

This research was performed by the support of Defense Acquisition Program Administration and Agency for Defense Development. The authors would like to express our appreciation to their supports.

8 Literature

- [1] Galle, L.F. and Erkel, van A.G.: "TNO-PML Developments of Blast Resistant Doors and Walls", *The 1st European Survivability Workshop*, Cologne, Germany, 2002.
- [2] Stark, S. and Sajdak, J.: "Design and Effectiveness Criteria for Blast Hardened Bulkhead Applications on Naval Combatants", *The 4th International Conference on Design and Analysis of Protective Structures*, Jeju, Republic of Korea, 2012.
- [3] Raymond, I.K.: *Tools for the formation of optimized X-80 Steel Blast Tolerant transverse bulkheads*, Master of Engineering Thesis in the University of New South Wales, 2001.
- [4] LSTC: *LS-DYNA User's Manual, Version 971 R6*, Livermore Soft Technology Corp., USA, 2012.